Applied Acoustics 74 (2013) 1271–1278

Contents lists available at SciVerse ScienceDirect

Applied Acoustics

journal homepage: www.elsevier.com/locate/apacoust

Harvesting low-frequency acoustic energy using multiple PVDF beam arrays in quarter-wavelength acoustic resonator

Bin Li [a], Andrew J. Laviage [a], Jeong Ho You [a,*], Yong-Joe Kim [b]

[a] Department of Mechanical Engineering, Southern Methodist University, Dallas, TX 75205, USA
[b] Department of Mechanical Engineering, Texas A&M University, College Station, TX 77843, USA

ARTICLE INFO

Article history:
Received 16 August 2012
Received in revised form 15 April 2013
Accepted 23 April 2013

Keywords:
Acoustic energy harvesting
Piezoelectric cantilever beam
Quarter-wavelength resonator

ABSTRACT

An acoustic energy harvester is introduced that uses a quarter-wavelength straight-tube acoustic resonator with polyvinylidene fluoride (PVDF) piezoelectric cantilever beams placed inside the resonator. When the tube is excited by an incident wave at its first acoustic eigenfrequency, an amplified acoustic resonant standing wave is developed inside the tube. The acoustic pressure gradient of the amplified standing wave then drives the vibration motion of the PVDF piezoelectric beams, generating electricity due to the direct piezoelectric effect. In order to maximize the amount of the harvested energy, each PVDF piezoelectric beam has been designed to have the same structural eigenfrequency as the acoustic eigenfrequency of the tube. With a single PVDF beam placed inside the tube, the harvested voltage and power become the maximum near the tube open inlet where the largest acoustic pressure gradient vibrates the PVDF beam. As the beam is moved to the tube closed end, the voltage and power gradually decrease due to the decreased acoustic pressure gradient. Multiple piezoelectric beams have been placed inside the tube with two different configurations: the aligned and zigzag configurations. With the zigzag configuration which has the more open path for acoustic air particle motions, the significant increases in the harvested voltage and power have been observed. Due to the interruption of acoustic air particle motion caused by the beams, it is found that placing PVDF beams near the closed tube end is not beneficial. The total output voltage of the piezoelectric beams increases linearly as the incident sound pressure increases.

1. Introduction

In the past decade, a variety of energy sources in environment including radiant (e.g., solar [1,2]), mechanical (e.g., wind [3,4] and vibration [5,6]), thermal [7,8] and biochemical [9,10] energy, have been investigated as potential sources for energy harvesting. Although there have been significant efforts in developing environmental energy harvesting technologies, our environment is still full of wasted and unused energy. Acoustic energy is one example of these currently wasted energies. Compared with other energy sources, insignificant efforts have been devoted to developing acoustic energy harvesting methods. Since acoustic energy is a clean, ubiquitous, and sustainable energy source and a significant amount of acoustic energy is available in some circumstances (for example, airports, construction sites, factory, etc.), it is of great interest to investigate acoustic energy harvesting mechanisms.

Horowitz et al. [11] first introduced a micromachined acoustic energy harvester using a Helmholtz resonator with a piezoelectric ring attached to one of the resonator walls. A maximum output power of ~0.1 nW was obtained with an incident sound pressure level (SPL) of 149 dB (referenced 20 μPa [12]) at 13.6 kHz. Liu et al. [13–15] developed an electromechanical Helmholtz resonator which utilized a uniform acoustic pressure in a resonator chamber to bend a piezoelectric back plate. The resonator was excited by an incident SPL of 160 dB at 2.6 kHz, generating a maximum output power of 30 mW which could be enough to supply energy to low power electronics. Kim et al. [16] also used a Helmholtz resonator in which a permanent magnet/coil system was driven by acoustic pressure to harvest airflow and aeroacoustic energy. An output voltage of 4 mV was measured with an input pressure of 0.2 kPa (i.e., 140 dB SPL) at 1.4 kHz. In addition to Helmholtz resonators, periodic structures have been used to confine acoustic waves [17–19]. Wu et al. [20–22] used a disordered structural pattern in a sonic crystal to trap acoustic waves and to amplify sound pressure. By placing a curved PVDF piezoelectric beam inside the disordered structural pattern, the amplified sound pressure excited the beam and an output power of ~35 nW was harvested from an incident wave with ~90 dB at 4.2 kHz. Lastly, piezoelectric zinc oxide nanowires were used to harvest ultrasonic waves to power nanodevices and nanosystems [23].

* Corresponding author. Tel.: +1 214 768 3126.
E-mail address: jyou@smu.edu (J.H. You).

0003-682X/$ - see front matter © 2013 Elsevier Ltd. All rights reserved.
http://dx.doi.org/10.1016/j.apacoust.2013.04.015

Most previous studies have focused on harvesting acoustic energy at relatively high frequencies ranged from a few kHz to MHz. However, sound sources available in everyday life contain predominantly low frequency components due to their lower spatial attenuation rates, compared with high frequency sound [24]. Therefore, it is necessary to develop an innovative mechanism to harvest low-frequency acoustic energy. In this article, a quarter-wavelength straight-tube acoustic resonator with PVDF piezoelectric cantilever beams is proposed to harvest acoustic energy from travelling sound waves at a low frequency. The length of the tube is 58 cm and its corresponding first acoustic eigenfrequency is 146 Hz. The harvesting frequency can be easily tuned by changing the tube length. When the tube is excited by an external sound wave at its eigenfrequency, a resonant standing wave is developed inside the tube. When PVDF cantilever beams are placed perpendicular to the tube axis, the resonant standing wave excites the vibration motion of the PVDF piezoelectric beams, resulting in the generation of electricity.

This paper is organized as follows. In Section 2, the acoustic resonant behavior of quarter-wavelength resonator and the mechanism to convert acoustic energy to electrical power are presented. Experimental apparatus and procedures are discussed in Section 3. In Section 4, the output voltage and power with a single PVDF beam and multiple PVDF beams are discussed. Conclusions are drawn in the last section.

2. Acoustic energy harvesting mechanism

2.1. Acoustic resonance of quarter-wavelength resonator

Acoustic resonators such as half-wavelength, quarter-wavelength, and Helmholtz resonators, as shown in Fig. 1, have been used for both sound augmentation in musical instruments [25] and noise attenuation in industrial applications, for example, ducts [26,27], buildings [28], fans [29], etc. When these resonators are excited by an incident wave at their acoustic resonant frequencies, acoustic energy is collected inside the resonators in a form of standing resonant waves. The efficiency of collecting acoustic energy inside half and quarter-wavelength resonators has been studied experimentally in terms of sound attenuation outside the resonators [30]. It was found that a quarter-wavelength resonator collects acoustic energy about three time more than a half-wavelength resonator at a given diameter and frequency. Compared with a Helmholtz resonator, a quarter-wave resonator requires less volume to collect the same amount of acoustic energy at a given frequency [30]. Therefore, a quarter-wavelength resonator is expected to be the best design amongst these resonators to collect acoustic energy in a closed space.

A typical Helmholtz resonator consists of a neck and a cavity as shown in Fig. 1a. For the first eigenmode, the air in the neck oscillates as a mass while the static air in the cavity undergoes compression and expansion as a spring. Including energy dissipations (e.g., the sound radiation from the open neck and the friction between air particles and resonator walls), the Helmholtz resonator can be modeled as a mass-spring-damper system [24]. Assuming the wavelength of an incident wave is much larger than the dimensions of Helmholtz resonator, the first eigenfrequency f_1 can be obtained from the lumped element model as [24,31]

$$f_1 = \frac{c_0}{2\pi}\sqrt{\frac{S}{lV}}, \tag{1}$$

where c_0 is the sound speed, S is the cross-sectional area of the neck, V is the cavity volume, and l is the effective neck length including the end corrections. When the resonator is excited at f_1, the sound pressure in the cavity is resonantly amplified. The amplification ratio A of the cavity pressure to the incident pressure is represented as [24]

$$A = \frac{p_{\text{cavity}}}{p_{\text{incident}}} = 2\pi\sqrt{\frac{l^3V}{S^3}}. \tag{2}$$

From Eqs. (1) and (2), in order to lower the eigenfrequency and increase the amplification ratio, a Helmholtz resonator with a large chamber volume and a long narrow neck is preferred. As shown in Eq. (2), however, the neck length and cross-sectional area predominate the cavity volume in the amplification ratio. Therefore, in designing a small harvester, it is desired to have a resonator with long and narrow dimensions, such as a quarter-wavelength tube resonator [32].

Unlike the Helmholtz resonator, a quarter-wavelength resonator shown in Fig. 1c cannot be modeled as lumped elements since its longitudinal dimension is not much smaller than the wavelength. In the quarter-wavelength resonator, the longitudinal particle velocity $u(z,t)$ and acoustic pressure $p(z,t)$ at the n-th resonant mode are represented as sinusoidal functions [33]

$$u(z,t) = u_0 \cos\frac{\pi(2n-1)z}{2L}\exp(i2\pi f_n t), \tag{3}$$

$$p(z,t) = p_0 \sin\frac{\pi(2n-1)z}{2L}\exp(i2\pi f_n t), \tag{4}$$

where L is the tube length which is equal to $(2n-1)\lambda/4$, z is the distance measured from the tube open inlet, f_n is the eigenfrequency, and n is the mode number, $n = 1, 2, 3,\ldots$ At the first eigenmode (i.e., $n = 1$), the tube length is equal to a quarter wavelength, $L = \lambda/4$. From Eqs. (3) and (4), the maximum magnitude of particle velocity u_0 occurs at the tube open inlet while the acoustic pressure reaches the maximum magnitude p_0 at the closed end of tube.

2.2. Acoustic energy conversion by piezoelectric beam inside tube resonator

When a clamped-free piezoelectric beam is placed inside the tube resonator, the spatially varying acoustic resonant pressure in Eq. (4) induces the pressure difference between each side of the beam as shown in Fig. 2. The pressure difference Δp drives the vibration motion of the piezoelectric beam at the frequency f_n, resulting in generating electricity by the 31 piezoelectric mode. When a beam is placed near the tube inlet where the pressure gradient is at the maximum, a large displacement of beam will generate a high voltage.

Output power from piezoelectric energy harvesters strongly depends on the electrical impedance of external circuit [15,20,34,35]. Most previous studies have focused on the optimized loading resistance and output power of a cantilever beam driven by a base excitation [34,36]. In this study, the optimized loading resistance and output power for a cantilever beam excited by acoustic pressure difference Δp are obtained as following. The equivalent circuit model for mechanical and electrical elements of a piezoelectric cantilever beam can be described by Kirchoff's Voltage Law (KVL) [34,37]

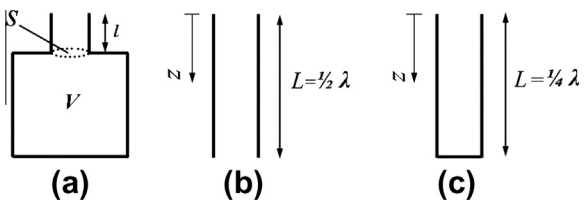

Fig. 1. Sketches of (a) Helmholtz, (b) half-wavelength, and (c) quarter-wavelength resonators.

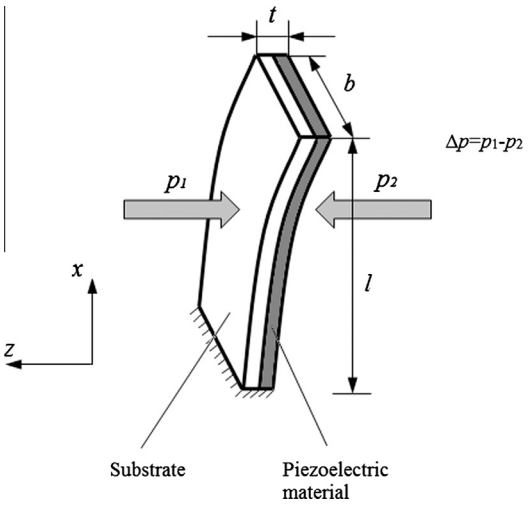

Fig. 2. Clamped-free unimorph piezoelectric cantilever beam vibrated by acoustic pressure difference.

$$\sigma_{\text{in}} = \sigma_i + \sigma_d + \sigma_s + \sigma_p, \tag{5}$$

where σ_{in} is an input stress and σ_i, σ_d, σ_s, and σ_p are the equivalent stresses to inertial, damping, stiffness, and piezoelectric elements, respectively. The input stress σ_{in} can be regarded as the average normal stress induced by bending moment $M_p(x)$ as

$$\sigma_{\text{in}} = \frac{1}{l}\int_0^l \frac{M_p(x)t_c}{I}dx, \tag{6}$$

where I is the moment of inertia, t_c is the distance from the neutral axis to the center of the piezoelectric layer. $M_p(x)$ is the bending moment generated by the acoustic pressure difference Δp. In order to obtain σ_i, σ_d, σ_s, and σ_p the cantilever beam with distributed mass under uniform acoustic pressure in Fig. 3a is simplified to the beam with a point mass under a concentrated force in Fig. 3b.

The equivalent point mass in Fig. 3b can be obtained by equating kinetic energy for both systems. The displacement for the cantilever beam with distributed mass under Δp is expressed as [38]

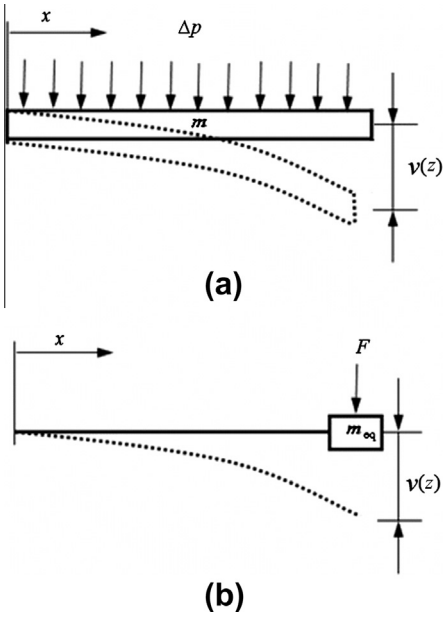

Fig. 3. Sketch for cantilever beam with (a) distributed mass and (b) point mass.

$$v(\tau,x) = \frac{bx^2(6l^2+4lx+x^2)}{24EI}\Delta p, \tag{7}$$

where E is the Young's modulus and b is width of the beam. A differential element dx contains kinetic energy as

$$dG_k = \frac{\dot{v}(\tau,x)^2}{2}\frac{mdx}{l}. \tag{8}$$

Kinetic energy can be obtained by integration over the beam length l as

$$G_k = \int_0^l dG_k = \frac{\dot{v}(\tau,l)^2}{2}0.257m. \tag{9}$$

Therefore, the equivalent point mass is $m_{eq} = 0.257m$. The induced stress to each element are given as

$$\sigma_i = \frac{m_{eq}}{c_1}\ddot{\delta}, \tag{10}$$

$$\sigma_d = \frac{\eta}{c_2}\dot{\delta}, \tag{11}$$

$$\sigma_s = E\delta, \tag{12}$$

$$\sigma_p = \frac{-dE}{t_p}V, \tag{13}$$

where δ is strain, t_p is the thickness of piezoelectric material, the damping coefficient is $\eta = 2\zeta\omega_n m_{eq}c_2/c_1$ with a damping ratio ζ and the geometric constants $c_1 = 3I/l^3$ and $c_2 = 3t_c/(2l^2)$. Substituting Eqs. (6), (10), (11), (12), (13) into Eq. (5) gives the magnitude of output voltage as a function of Δp as

$$V_{mag.} = \frac{\omega_n RC_p dt_p/\varepsilon}{\sqrt{R^2C_p^2\omega_n^2(4\zeta^2+k^2)+4\zeta^2+4\zeta k^2\omega_n RC_p}}\left(\frac{t_c l^2 b}{6I}\right)\Delta p, \tag{14}$$

where k is the piezoelectric coupling coefficient, d is the piezoelectric constant, C_p is the piezoelectric capacitance, R is the loading resistance, and ε is the permittivity. Then, the output electric power P is given as

$$P = \frac{V_{mag.}^2}{R} = \frac{(\omega_n dt_p/\varepsilon)^2 RC_p^2}{\omega_n^2R^2C_p^2(4\zeta^2+k^4)+4\zeta^2+4k^2\zeta\omega_n RC_p}\left(\frac{t_c l^2 b}{6I}\Delta p\right)^2. \tag{15}$$

The amount of harvested power can be maximized when $\partial P/\partial R = 0$. The optimized resistance can be obtained as

$$R_{opt} = \frac{1}{\omega_n C_p}\frac{2\zeta}{\sqrt{4\zeta^2+k^4}}. \tag{16}$$

3. Experiments

A quarter-wavelength acoustic tube resonator has been fabricated using 1/2 in. thick polycarbonate plates as shown in Fig. 4. The tube is 58 cm long with a uniform rectangular cross-section of 4 cm × 5 cm. Thick acoustical sealing caulk is applied between the gaps of the polycarbonate panels to minimize sound leakage. A premium powered loudspeaker (Audioengine 5 by *Audioengine*) driven by a data acquisition system (DAQ) NI-PCI 6289 is used to generate an incident sound wave. Quarter-inch condenser microphones (377C10 by *PCB Piezotronics*) powered by a sensor signal conditioner (482C05 by *PCB Piezotronics*) are used to measure acoustic pressures at various positions along the tube.

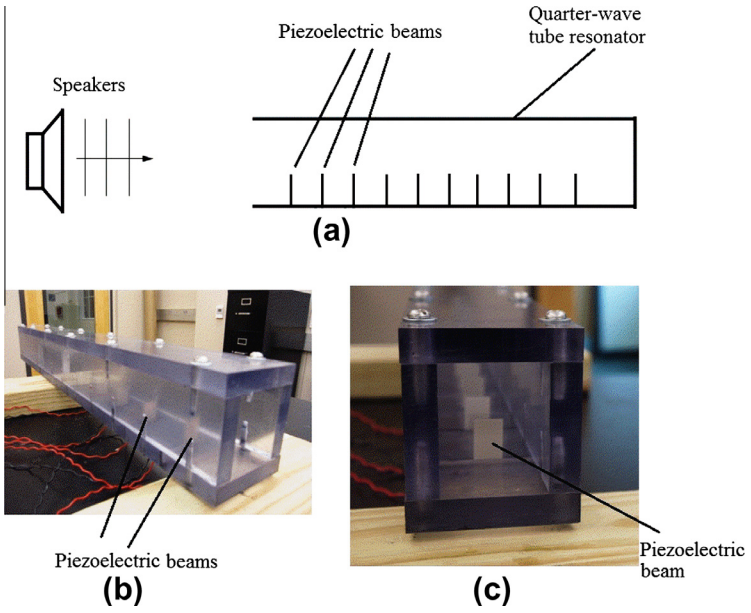

Fig. 4. (a) Sketch of experimental setup and (b) perspective and (c) front views of quarter-wavelength tube resonator with PVDF piezoelectric beam array. Thick sealing caulk is not shown here.

In order to convert the acoustic energy inside the tube resonator, unimorph polyvinylidene fluoride (PVDF) piezoelectric cantilever beams (LDT-028k by *Measurement Specialties*) have been placed along the tube as shown in Fig. 4a. Each piezoelectric beam has been designed to have the same structural eigenfrequency as the acoustic eigenfrequency of the tube. Dimensions of piezoelectric beam are 2 cm in length, 1.61 cm in width, and 0.2 mm in thickness. The unimorph piezoelectric beam consists of a 30 μm thick PVDF film (14%), a 127 μm thick polyester laminate (62%), and an adhesive layer (24%). The bottom panel of the tube consists of several polycarbonate blocks which clamp the thin PVDF beams. The material properties of the PVDF films are provided in Table 1.

4. Results

4.1. Amplified resonant pressure in quarter-wavelength tube resonator

In order to verify the acoustic eigenmodes of tube resonator, the tube is excited by an incident sound of 100 dB and acoustic pressure is measured at various positions along the tube. Fig. 5 shows the magnitudes of the first three acoustic pressure eigenmodes normalized by the incident pressure magnitude along the tube. The first three eigenfrequencies are measured as $f_1 = 146$ Hz, $f_2 = 439$ Hz, and $f_3 = 734$ Hz. The measured resonant acoustic pressures are well represented by the sinusoidal functions in Eq. (4) with the maximum magnitudes at the closed end of the tube. In a quarter-wavelength resonator, the amplification ratio can be defined as a ratio of the maximum pressure inside tube to the incident sound pressure p_{incident}. As shown in Fig. 5, the largest amplification ratio is obtained as 59.1 for the first eigenmode and decreases as the mode number increases: 42.2 and 23.3 at the second and third eigenmodes, respectively. It suggests that the most acoustic energy is accumulated inside the tube at the first eigenmode, which is consistent with the results from Ref. [30].

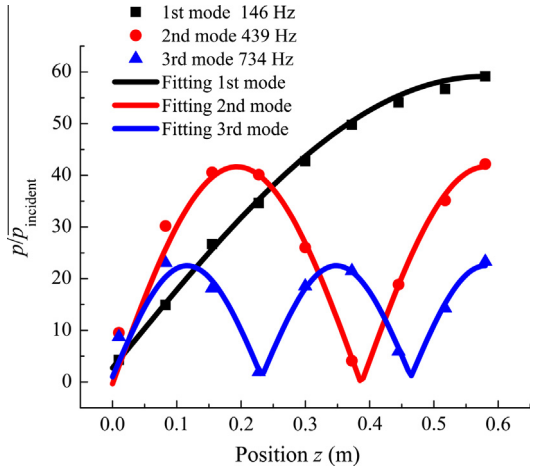

Fig. 5. Magnitudes of normalized first three acoustic pressure eigenmodes along 58 cm long straight tube with rectangular cross-section of 4 cm × 5 cm. The tube has the open inlet at $z = 0$ and the closed end at $z = 58$ cm.

Table 1
Material properties of PVDF piezoelectric beams (LDT-028k by *Measurement*).

Description and symbol	Value
Piezoelectric constant, d_{31}	23 pC/N
Relative permittivity, $\varepsilon/\varepsilon_0$	12–13
Young's modulus, E	2–4 GPa
Capacitance, C_p	5.5 nF
Coupling factor, k	0.12
Damping ratio, ζ	0.05

4.2. Acoustic energy harvesting using single piezoelectric beam

A single PVDF beam has been placed at various positions inside the tube as shown in Fig. 6a. The first position *A* is located at 5 cm from the tube inlet and additional positions are set at 5 cm increments. The quarter-wavelength acoustic energy harvester is excited by an incident wave of 100 dB at the first eigenfrequency $f_1 = 146$ Hz. Fig. 6b shows the output voltage and power generated by a single PVDF beam placed from positions *A* to *J*. A maximum output voltage of 0.105 V is measured when the beam is placed at the position *A* near the inlet of the tube. As the PVDF beam moves toward the tube closed end, the output voltage decreases

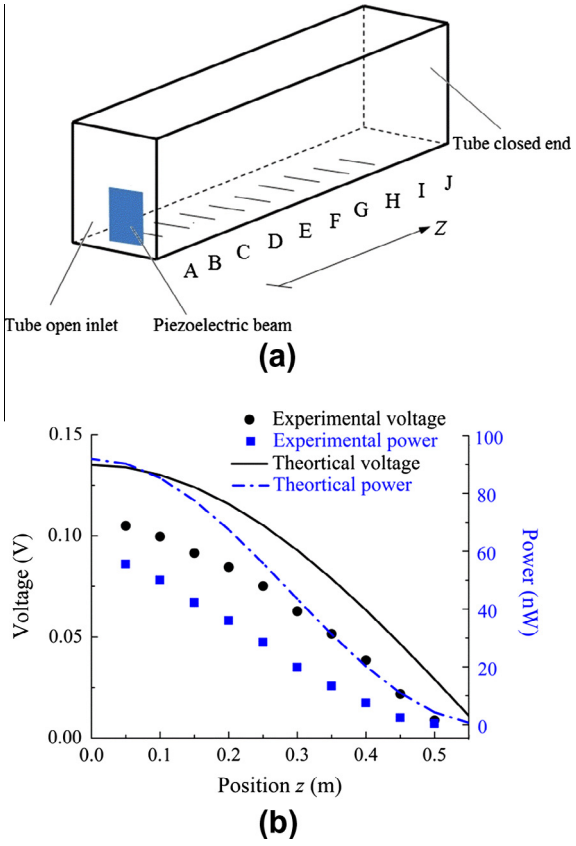

Fig. 6. (a) Sketch of quarter-wavelength tube resonator with single PVDF beam placed inside tube resonator and (b) experimental and theoretical output voltage and power by single PVDF beam at various positions along the tube resonator with the incident sound wave of 100 dB at 146 Hz.

gradually. This result is in line with the particle velocity u in (3), which is proportional to the pressure gradient. Since the PVDF beam is placed in the spatially fluctuating pressure field, the pressure difference across the beam thickness causes the beam to bend along the z-direction, resulting in voltage generation. When the PVDF beam is placed near the tube inlet, where the pressure gradient is at the maximum, the largest output voltage is obtained by a large beam deflection. When the beam is placed near the tube closed end, the small pressure gradient induces a small beam deflection, although the pressure magnitude is at the maximum at the tube closed end.

From Eq. (4), assuming the pressure difference across the beam as $\Delta p = p_0[\sin(\pi(z_B + t_B/2)/(2L)) - \sin(\pi(z_B - t_B/2)/(2L))]$ where t_B and z_B are the thickness and position of piezoelectric beam respectively, the voltage and power can be calculated from Eqs. (14) and (15) and are shown in Fig. 6b. The discrepancy between the experimental data and calculated results might be from neglecting the acoustic-structural interaction in the theoretical calculations. The actual driving force by the acoustic standing wave in the closed space of tube is different from the pressure difference of acoustic eigenmode which does not account for the presence of beams. It is analogous to the drag coefficient which relates a fluidic dynamic force with a drag force exerting on an immersed solid body in a fluid flow [39]. Further investigations are needed to understand the fluidic–acoustic–structural interaction in a closed space for better estimations.

4.3. Acoustic energy harvesting using multiple piezoelectric beams

In order to increase the output voltage and power, multiple PVDF beams have been placed in the tube. In this study, the beams have been placed in two different configurations: aligned and zigzag configurations. In the aligned configuration, all PVDF beams are placed along the centerline of tube as shown in Fig. 7a. In the zig-

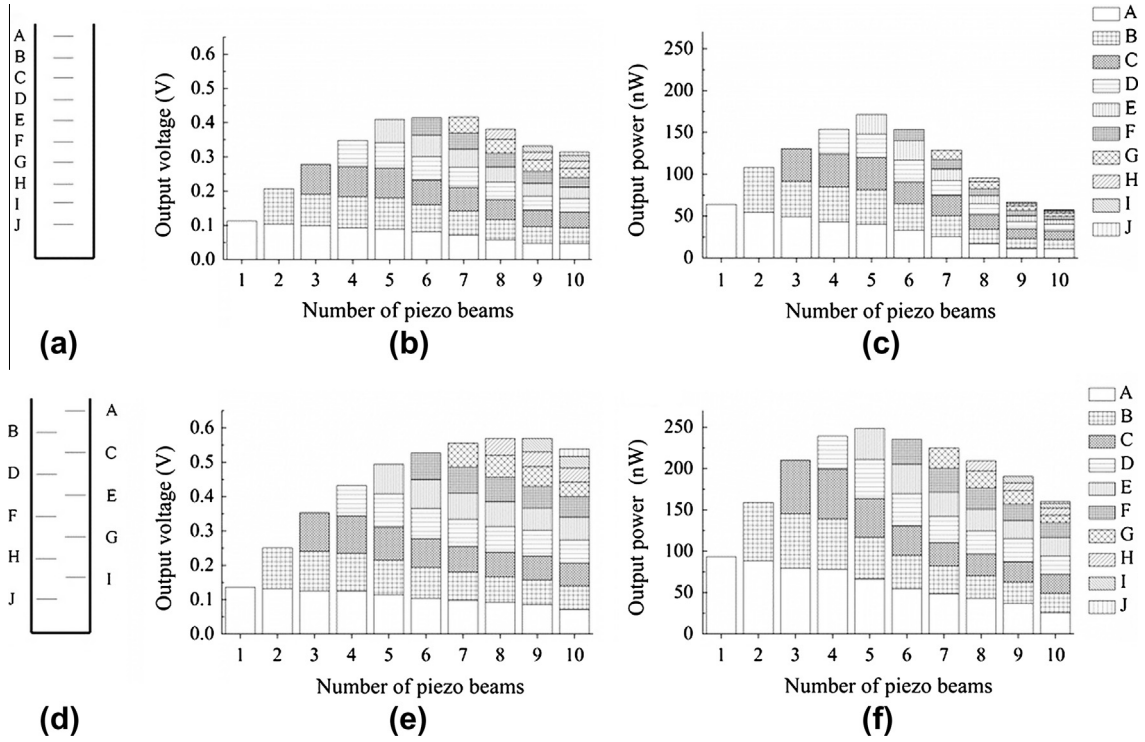

Fig. 7. Sketches of (a) aligned and (d) zigzag configurations, output voltages from (b) aligned and (e) zigzag configurations, and power from (c) aligned and (f) zigzag configurations with the incident sound wave of 100 dB at 146 Hz. For both the configurations, the spacing between beams along the tube axis is 5 cm.

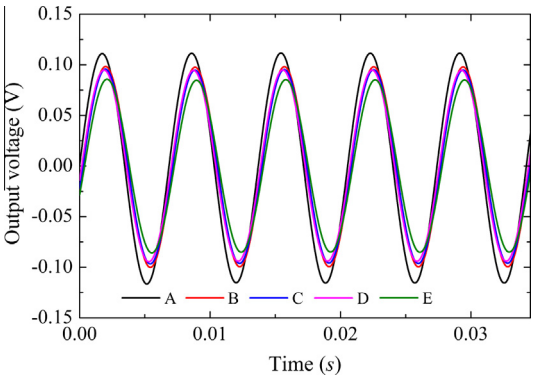

Fig. 8. Output voltage from five PVDF beams placed at positions *A* to *E* in aligned configuration.

zag configuration, the PVDF beams are placed in a zigzag pattern as shown in Fig. 7d. For both the configurations, the spacing between beams along the longitudinal tube axis is 5 cm. The output voltage with the aligned configuration is shown in Fig. 7b as a function of the number of piezoelectric beams placed in the tube. Piezoelectric beams are placed in the tube starting from the first position *A* near the open inlet to the last position *J* near the closed end. For example, the number of piezoelectric beams equal to 3 indicates that three beams are placed at the positions of *A*, *B*, and *C*. The voltage from each piezoelectric beam has been measured simultaneously and the total voltage is obtained by the summation of voltage from each beam assuming that all beams are connected in series.

For the aligned configuration as shown in Fig. 7b, the total output voltage increases as the number of beams increases until seven PVDF beams are placed at the positions *A* to *G*. A maximum total output voltage of 0.417 V has been measured. In addition to the seven beams at *A* through *G*, one or more additional beams at the positions *H* to *J* reduces the total output voltage. This is caused by the alteration of the acoustic resonance due to the additional beams near the tube closed end. In order to harvest more acoustic energy available in the resonator, it is desired to place more PVDF beams inside the tube. However, the presence of the beams in the tube reduces the acoustic resonant pressure by interrupting the air particle motion along the tube. This effect can also be seen in the case of the two beams at *A* and *B*. Comparing the first and second bars of Fig. 7b, the additional beam at the position *B* in addition to the beam at *A*, has decreased the voltage generated by the beam at *A*. Increasing the number of beams keeps reducing the voltage generated from each beam as shown in Fig. 7b.

To reduce the interference between the beams and air motion, the PVDF beams are placed in a zigzag pattern as shown in Fig. 7d. This configuration has more open path for air motion than the aligned configuration. The total output voltage in this zigzag configuration increases until nine PVDF beams are placed at the positions *A* through *I* (see Fig. 7d). The maximum voltage has been increased by 36.7% from 0.417 V to 0.570 V when compared with the aligned configuration in Fig. 7b. Also, the attenuation of the voltage generated by the first beam at *A* in the zigzag configuration is less than that in the aligned configuration. It can be concluded that the interference between the beams and air motion critically limits the maximum number of beams to obtain the maximum voltage.

From the measured voltage for each beam, the total power can be obtained as the summation of power from each beam. The estimated amounts of power using the aligned and zigzag configurations are shown in Fig. 7c and f, respectively. The maximum total power using the zigzag configuration is 248.5 nW, 45% higher than the maximum 171.4 nW of the aligned configuration. For both

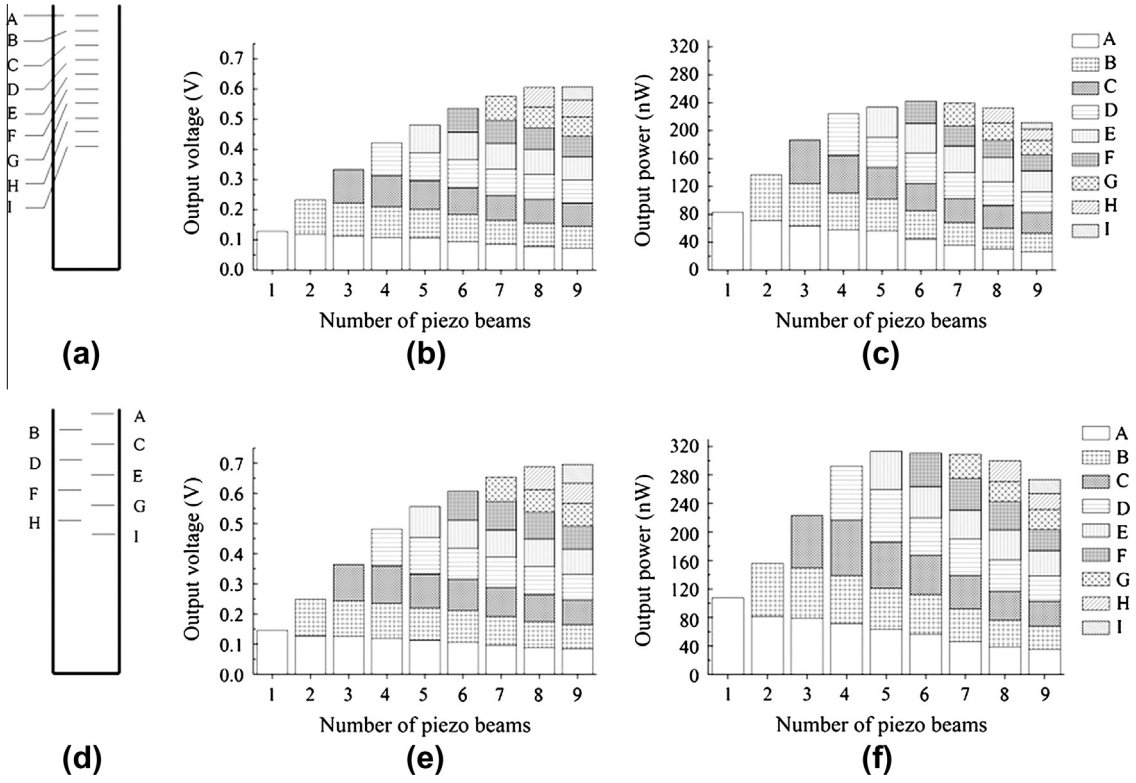

Fig. 9. Sketches of (a) aligned and (d) zigzag configurations with piezoelectric beams placed in the first half of tube, output voltages from (b) aligned and (e) zigzag configurations, and power from (c) aligned and (f) zigzag configurations with the incident sound wave of 100 dB at 146 Hz. For both the configurations, the spacing between beams along the tube axis is 2.5 cm.

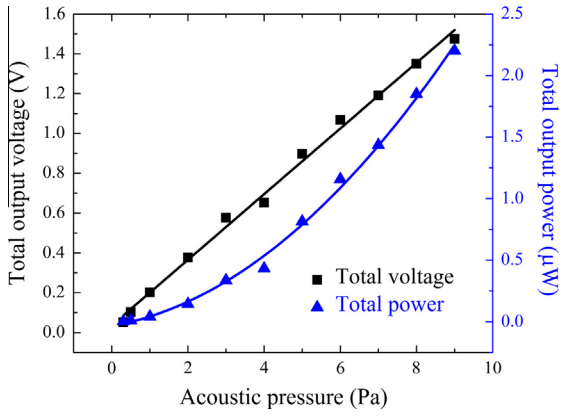

Fig. 10. Effects of incident acoustic pressure on total output voltage and power using five PVDF beams placed at the positions A (x = 2.5 cm) through E (x = 12.5 cm) in the zigzag configuration of Fig. 9d.

beam configurations, the number of beams that generate the maximum power is five, which is smaller than that for the maximum voltage. In terms of the total power represented by the summation of V^2/R from each beam, placing more piezoelectric beams also increases the total resistance. Therefore, placing the beams near the closed tube end, where the output voltage is relatively small, reduces the total power due to the increased resistance.

Fig. 8 shows the measured voltage from each piezoelectric beam in time domain when five piezoelectric beams are placed inside the tube resonator at the positions A to E in the aligned configuration (see Fig. 7a). It can be seen that the output voltages from individual piezoelectric beams are almost in the same phase, which indicates that all beams are vibrating in phase at their structural resonance.

Since placing additional PVDF beams near the tube closed end decreases the total power, the PVDF beams are placed only in the first half of the tube with the increased beam density as shown in Fig. 9a and d for the aligned and zigzag configurations, respectively. The first position A is located at 2.5 cm from the tube inlet and additional positions are set at 2.5 cm increments in order to fill the half of the tube. The maximum output voltage increases significantly from 0.417 V and 0.570 V to 0.607 V and 0.696 V for the aligned and zigzag configurations, respectively. There are also significant increases in the maximum total power from 171.4 nW and 248.5 nW to 242.4 nW and 313.3 nW (45% and 26% increments) in the aligned and zigzag configurations, respectively. The corresponding power density is 0.0157 μW/cm^2 at 100 dB SPL which is significantly higher than the previous acoustic energy harvesters [11,20,21], even at the lower operating frequency.

Fig. 10 shows the output voltage and power as a function of incident acoustic pressure using the five PVDF beams placed at the positions A (x = 2.5 cm) through E (x = 12.5 cm) in the zigzag configuration of Fig. 9d. The output voltage is linearly proportional to the incident acoustic pressure, which confirms that the driving force of beam deflections is the acoustic pressure gradient of resonant standing waves. The voltage of 1.48 V is measured with an incident pressure of 9 Pa (i.e., SPL = 110 dB). The corresponding estimated power is 2.2 μW and the power density of 0.11 μW/cm^2 is obtained at SPL = 110 dB.

5. Conclusion

The 58 cm long quarter-wavelength tube resonator with various piezoelectric beam array configurations has been studied to harvest low-frequency acoustic energy. The amplification ratio of 59.1 has been measured at the first eigenmode (f_1 = 146 Hz), and it decreases to 42.2 at f_2 = 439 Hz and 23.3 at f_3 = 734 Hz. In order to convert the first-eigenmode acoustic energy inside the tube, PVDF piezoelectric beams have been placed along the tube axis. With a single PVDF beam placed inside the tube, the voltage and power become the maximum near the tube open inlet where the largest acoustic pressure gradient vibrates the beam. The voltage and power gradually decrease as the beam is moved to the tube closed end. With the incident wave of 100 dB at f_1 = 146 Hz, the single PVDF beam near the tube inlet has generated the voltage of 0.105 V, which corresponds to the power of 55.6 nW. In order to increase the output voltage, multiple piezoelectric beams have been placed inside the tube with the aligned and zigzag configurations. Compared with the aligned configuration, the zigzag configuration significantly increases the voltage and power due to the more open path for acoustic air particle motion. It is observed that the number of beams to generate the maximum voltage is limited by the interruption of acoustic air particle motion caused by the beams. The maximum voltage and power have been obtained with beams placed in the first half of the tube resonator in the zigzag configuration, resulting in 0.696 V and 0.31 μW at the incident SPL of 100 dB. The voltage increases linearly with the incident sound pressure. At the incident SPL of 110 dB, the voltage of 1.48 V has been measured which corresponds to the power of 2.2 μW with the power density of 0.11 μW/cm^2.

References

[1] Dondi D, Bertacchini A, Brunelli D, Larcher L, Benini L. Modeling and optimization of a solar energy harvester system for self-powered wireless sensor networks. IEEE T Ind Electron 2008;55:2759–66.
[2] Abrams ZR, Niv A, Zhang X. Solar energy enhancement using down-converting particles: a rigorous approach. J Appl Phys 2011;109:114905.
[3] Ovejas VJ, Cuadras A. Multimodal piezoelectric wind energy harvesters. Smart Mater Struct 2011;20:085030.
[4] Jung HJ, Kim IH, Jang SJ. An energy harvesting system using the wind-induced vibration of a stay cable for powering a wireless sensor node. Smart Mater Struct 2011;20:075001.
[5] Jo SE, Kim MS, Kim YJ. A resonant frequency switching scheme of a cantilever based on polyvinylidene fluoride for vibration energy harvesting. Smart Mater Struct 2012;21:015007.
[6] Gao XT, Shih WH, Shih WY. Vibration energy harvesting using piezoelectric unimorph cantilevers with unequal piezoelectric and nonpiezoelectric lengths. Appl Phys Lett 2010;97:233503.
[7] Knight C, Davidson J. Thermal energy harvesting for wireless sensor nodes with case studies. Adv Wireless Sensors Sensors Networks 2010;64:221–42.
[8] Cuadras A, Gasulla M, Ferrari V. Thermal energy harvesting through pyroelectricity. Sensor Actuat A – Phys 2010;158:132–9.
[9] Hansen BJ, Liu Y, Yang R, Wang ZL. Hybrid nanogenerator for concurrently harvesting biomechanical and biochemical energy. ACS Nano 2010;4:3647–52.
[10] Yang R, Qin Y, Li C, Zhu G, Wang ZL. Converting biomechanical energy into electricity by a muscle-movement-driven nanogenerator. Nano Lett 2009;9:1201–5.
[11] Horowitz SB, Sheplak M, Cattafesta LN, Nishida T. A MEMS acoustic energy harvester. J Micromech Microeng 2006;16:S174–81.
[12] Manglarotty RA. Acoustic-lining concepts and materials for engine ducts. J Acoust Soc Am 1973;48:783–94.
[13] Liu F, Phipps A, Horowitz S, Ngo K, Cattafesta L, Nishida T, et al. Acoustic energy harvesting using an electromechanical Helmholtz resonator. J Acoust Soc Am 2008;123:1983–90.
[14] Liu F, Horowitz S, Nishida T, Cattafesta L, Sheplak M. A multiple degree of freedom electromechanical Helmholtz resonator. J Acoust Soc Am 2007;122:291–301.
[15] Phipps A, Liu F, Cattafesta L, Sheplak M, Nishida T. Demonstration of a wireless, self-powered, electroacoustic liner system. J Acoust Soc Am 2009;125:873–81.
[16] Kim SH, Ji CH, Galle P, Herrault F, Wu X, Lee JH, et al. An electromagnetic energy scavenger from direct airflow. J Micromech Microeng 2009;19:094010.
[17] Khelif A, Mohammadi S, Eftekhar AA, Adibi A, Aoubiza B. Acoustic confinement and waveguiding with a line-defect structure in phononic crystal slabs. J Appl Phys 2010;108:084515.
[18] Duhring MB, Laude V, Khelif A. Energy storage and dispersion of surface acoustic waves trapped in a periodic array of mechanical resonators. J Appl Phys 2009;105:093504.
[19] Vorobiev A, Gevorgian S, Loffler M, Olsson E. Correlations between microstructure and Q-factor of tunable thin film bulk acoustic wave. J Appl Phys 2011;110:054102.
[20] Wu LY, Chen LW, Liu CM. Acoustic energy harvesting using resonant cavity of a sonic crystal. Appl Phys Lett 2009;95:013506.

[21] Wang WC, Wu LY, Chen LW, Liu CM. Acoustic energy harvesting by piezoelectric curved beams in the cavity of a sonic crystal. Smart Mater Struct 2010;19:045016.
[22] Wu LY, Chen LW, Liu CM. Acoustic pressure in cavity of variously sized two-dimensional sonic crystals with various filling fractions. Phys Lett A 2009;373:1189–95.
[23] Wang XD, Song JH, Liu J, Wang ZL. Direct-current nanogenerator driven by ultrasonic waves. Science 2007;316:102–5.
[24] Blackstock D. Fundamentals of physical acoustic, A Wiley-Interscience. New York Publication; 2000.
[25] Bork I. Practical tuning of xylophone bars and resonators. Appl Acoust 1995;46:103–27.
[26] Tang SK. On sound transmission loss across a Helmholtz resonator in a low Mach number flow duct. J Acoust Soc Am 2010;127:3519–25.
[27] Wang ZG, Lee SH, Kim CK, Park CM, Nahm K, Nikitov SA. Acoustic wave propagation in one-dimensional phononic crystals containing Helmholtz resonators. J Appl Phys 2008;103:064907.
[28] Field CD, Fricke FR. Theory and applications of quarter-wave resonators: a prelude to their use for attenuating noise entering buildings through ventilation openings. Appl Acoust 1998;53:117–32.
[29] Koopmann GH, Neise W. The use of resonators to silence centrifugal blowers. J Sound Vib 1982;82:17–27.
[30] Sohn CH, Park JH. A comparative study on acoustic damping induced by half-wave, quarter-wave, and Helmholtz resonators. Aerosp Sci Technol 2011;15:606–14.
[31] Chen KT, Chen YH, Lin KY, Weng CC. The improvement on the transmission loss of a duct by adding Helmholtz resonators. Appl Acoust 1998;54:71–82.
[32] Li B, You JH. Harvesting ambient acoustic energy using acoustic resonators. Proc Meet Acoust 2011;12:065001.
[33] Alster M. Improved calculation of resonant frequencies of Helmholtz resonators. J Sound Vib 1972;24:63–85.
[34] Roundy S, Wright PK. A piezoelectric vibration based generator for wireless electronics. Smart Mater Struct 2004;13:1131–42.
[35] Koyama D, Nakamura K. Electric power generation using vibration of a polyurea piezoelectric thin film. Appl Acoust 2010;71:439–45.
[36] Erturk A, Inman DJ. An experimentally validated bimorph cantilever model for piezoelectric energy harvesting from base excitation. Smart Mater Struct 2009;18:025009.
[37] Roundy S, Wright RK, Rabaey JM. Energy scavenging for wireless sensor networks with special focus on vibration. Norwell: Kluwer academic publishers; 2003.
[38] Hibbeler R. Mechanics of Materials. New Jersey: Pearson Prentice Hall; 2008.
[39] Munson B, Young D, Okiishi T. Fundamentals of Fluid Mechanics. Okiishi: John Wiley & Sons; 1998.